Food-grade titanium dioxide translocates across the buccal mucosa in pigs and induces genotoxicity in an in vitro model of human oral epithelium

Julien Vignard, Aurelie Pettes-Duler, Eric Gaultier, Christel Cartier, Laurent Weingarten, Antje Biesemeier, Tatjana Taubitz, Philippe Pinton, Cecilia Bebeacua, Laurent Devoille, et al.

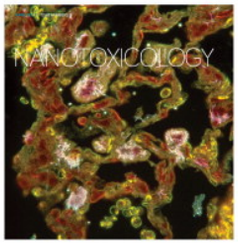

Nanotoxicology

ISSN: (Print) (Online) Journal homepage: https://www.tandfonline.com/loi/inan20

Food-grade titanium dioxide translocates across the buccal mucosa in pigs and induces genotoxicity in an *in vitro* model of human oral epithelium

Julien Vignard, Aurelie Pettes-Duler, Eric Gaultier, Christel Cartier, Laurent Weingarten, Antje Biesemeier, Tatjana Taubitz, Philippe Pinton, Cecilia Bebeacua, Laurent Devoille, Jacques Dupuy, Elisa Boutet-Robinet, Nicolas Feltin, Isabelle P. Oswald, Fabrice H. Pierre, Bruno Lamas, Gladys Mirey & Eric Houdeau

To cite this article: Julien Vignard, Aurelie Pettes-Duler, Eric Gaultier, Christel Cartier, Laurent Weingarten, Antje Biesemeier, Tatjana Taubitz, Philippe Pinton, Cecilia Bebeacua, Laurent Devoille, Jacques Dupuy, Elisa Boutet-Robinet, Nicolas Feltin, Isabelle P. Oswald, Fabrice H. Pierre, Bruno Lamas, Gladys Mirey & Eric Houdeau (2023): Food-grade titanium dioxide translocates across the buccal mucosa in pigs and induces genotoxicity in an *in vitro* model of human oral epithelium, Nanotoxicology, DOI: 10.1080/17435390.2023.2210664

To link to this article: https://doi.org/10.1080/17435390.2023.2210664

NANOTOXICOLOGY
https://doi.org/10.1080/17435390.2023.2210664

Taylor & Francis
Taylor & Francis Group

ARTICLE

OPEN ACCESS Check for updates

Food-grade titanium dioxide translocates across the buccal mucosa in pigs and induces genotoxicity in an *in vitro* model of human oral epithelium

Julien Vignard[a], Aurelie Pettes-Duler[a], Eric Gaultier[a], Christel Cartier[a], Laurent Weingarten[b], Antje Biesemeier[c], Tatjana Taubitz[c], Philippe Pinton[a], Cecilia Bebeacua[d], Laurent Devoille[e], Jacques Dupuy[a], Elisa Boutet-Robinet[a], Nicolas Feltin[e], Isabelle P. Oswald[a], Fabrice H. Pierre[a], Bruno Lamas[a], Gladys Mirey[a] and Eric Houdeau[a]

[a]Toxalim UMR1331 (Research Centre in Food Toxicology), Toulouse University, INRAE, ENVT, INP-Purpan, UPS, Toulouse, France; [b]Centre de MicroCaractérisation Raimond Castaing, UAR 3623, Toulouse, France; [c]Luxembourg Institute of Science and Technology (LIST), Materials Research and Technology (MRT), Advanced Instrumentation for Ion Nano-Analytics (AINA), Esch-sur-Alzette, Luxembourg; [d]ETH Zurich, Zurich, Switzerland; [e]Department of materials, LNE, Trappes, France

ABSTRACT

The whitening and opacifying agent titanium dioxide (TiO_2) is used worldwide in various foodstuffs, toothpastes and pharmaceutical tablets. Its use as a food additive (E171 in EU) has raised concerns for human health. Although the buccal mucosa is the first area exposed, oral transmucosal passage of TiO_2 particles has not been documented. Here we analyzed E171 particle translocation *in vivo* through the pig buccal mucosa and *in vitro* on human buccal TR146 cells, and the effects on proliferating and differentiated TR146 cells. In the buccal floor of pigs, isolated TiO_2 particles and small aggregates were observed 30 min after sublingual deposition, and were recovered in the submandibular lymph nodes at 4 h. In TR146 cells, kinetic analyses showed high absorption capacities of TiO_2 particles. The cytotoxicity, genotoxicity and oxidative stress were investigated in TR146 cells exposed to E171 in comparison with two TiO_2 size standards of 115 and 21 nm in diameter. All TiO_2 samples were reported cytotoxic in proliferating cells but not following differentiation. Genotoxicity and slight oxidative stress were reported for the E171 and 115 nm TiO_2 particles. These data highlight the buccal mucosa as an absorption route for the systemic passage of food-grade TiO_2 particles. The greater toxicity on proliferating cells suggest potential impairement of oral epithelium renewal. In conclusion, this study emphasizes that buccal exposure should be considered during toxicokinetic studies and for risk assessment of TiO_2 in human when used as food additive, including in toothpastes and pharmaceutical formulations.

ARTICLE HISTORY
Received 18 January 2023
Revised 3 April 2023
Accepted 1 May 2023

KEYWORDS
Oral mucosa; titanium dioxide; nanoparticles; cytotoxicity; genotoxicity

Introduction

Due to the rapid expansion of nanotechnologies and the daily increasing use of nanomaterials in consumer products, there is a growing need to assess the toxicological risks of these materials on human health. Such concern increases when nanoparticles (NPs) are found in food additives and coating substances or are included in food packaging, leading to chronic oral exposure to NPs for consumers. Among these agents, food-grade titanium dioxide (TiO_2) is commonly used as a food additive worldwide, and is referred to as E171 in European Union. It is used *ad quantum satis* as a whitening and brightening agent in a variety of food products (confectionary and bakery commodities, white sauces and icing), as beverage whiteners and in personal care products such as toothpaste but also in pharmaceutical tablets (Bischoff et al. 2020; European Medicines Agency 2021; Palugan et al. 2022). For these uses, large amounts of TiO_2 powders are produced and are composed of particles of various sizes ranging from 20 to 400 nm, and up to 55% of them by number are NPs (diameter $<$100 nm) (Weir et al. 2012; Bettini et al. 2017;

CONTACT Julien Vignard julien.vignard@inrae.fr; Eric Houdeau eric.houdeau@inrae.fr INRAE Toxalim UMR 1331, 180 Chemin de Tournefeuille, Toulouse 31027, France

Supplemental data for this article can be accessed online at https://doi.org/10.1080/17435390.2023.2210664.

Dorier et al. 2017; Guillard et al. 2020). Focusing on only food origin, depending on the exposure scenario and population groups, the mean dietary intake in humans has been estimated to range from 0.03 mg of TiO_2/kg of body weight (bw)/day (d) in infants to 11.5 mg/kg bw/d in children under 10 years of age and up to 6.7 mg/kg bw/d for older groups (Younes et al. 2021). Concerning TiO_2 fate and organ toxicity, chronic exposure to TiO_2 has been reported to result in particle accumulation in human tissues, including the intestine, liver, spleen and kidney (Heringa et al. 2018; Peters et al. 2020) as well as in the placenta (Guillard et al. 2020). Investigations in rodent models and cell lines have raised concerns regarding genotoxicity, inflammation and oxidative stress (Bischoff et al. 2020) as well as the potential for E171 to initiate and promote preneoplastic lesions in the rat colon (Bettini et al. 2017; Medina-Reyes et al. 2020). In mice, daily exposure to food-grade TiO_2 in a colitis-associated colorectal cancer model also exacerbated tumor formation in the colon (Urrutia-Ortega et al. 2016).

Because of these potential hazards to humans, a ban on the use of E171 in foods has been implemented in the EU in 2022 (Commission Regulation (EU))) 2022), while TiO_2 remains approved in the pharmaceutical industry for oral formulations among other applications (cosmetics, toothpaste), and is still allowed in the food chain outside the EU. To date, risk assessments of TiO_2 by food and consumer product safety authorities has been mainly based on the assumption that orally ingested TiO_2-NPs are mainly absorbed by the intestine (EFSA Panel on Food Additives and Nutrient Sources added to Food (ANS))) 2016; Heringa et al. 2016; Younes et al. 2021). However, oral toxicokinetic studies have estimated that only 0.02% to 0.6% of the administered TiO_2 dose is absorbed at the intestinal level including in humans (Cho et al. 2013; Jones et al. 2015; EFSA Panel on Food Additives and Nutrient Sources added to Food (ANS))) 2016; Kreyling et al. 2017). When considering the oral uptake of xenobiotics, the buccal cavity represents the first area of exposure and thus the first possible systemic delivery portal. In the context of food additives, the cellular uptake and toxicity potential of food-grade TiO_2 has not been addressed in a buccal model, although the mouth should be considered to be the body region exposed to a higher load of TiO_2-NPs once they are released from the food matrix. Indeed, with the example of chewing gum, among other sweets in which TiO_2 is used as a surface coloring agent (Chen et al. 2013; Fiordaliso et al. 2018), TiO_2 particles may be easily released from the gum (Chen et al. 2013; Dudefoi et al. 2018), dispersed in the saliva, and rapidly come into contact with the buccal epithelium. Similar scenarios can be drawn in other food categories where TiO_2 is added to a liquid or semiliquid matrix including ice cream, sauces and drinks (Younes et al. 2021), or when used as an opacifier in pharmaceutical tablets coating formulations (Palugan et al. 2022).

Given the lack of information on the food additive E171, the potential of toxicity of TiO_2 at the mouth level has been addressed in few studies using non-food NP models of known sizes. In a porcine *ex vivo* model of the buccal cavity exposed to nanomodels, five TiO_2-NPs with distinct physicochemical properties were shown to permeate the mucosa layer and penetrate the oral epithelium (Teubl et al. 2015a; Teubl et al. 2015b). Mucosal penetration and intracellular outcome depend on particle size and surface hydrophilicity/hydrophobicity. Indeed, TiO_2-NPs penetrated the entire buccal epithelium and the connective tissue, except for the nanomaterials with the smallest particle size (i.e., $<$30 nm), which were unable to reach the lower epithelium (Teubl et al. 2015a). Such size-dependent permeation into the deeper part of the buccal mucosa has already been observed for the penetration of neutral polystyrene NPs (Teubl et al. 2013). Moreover, hydrophilic TiO_2-NPs appeared to be freely distributed in the cytoplasm as small aggregates whereas their hydrophobic counterparts were encapsulated into vesicle structures. Regardless of their cellular distribution, none of the tested TiO_2-NPs were shown to affect cell viability or membrane integrity in the TR146 human buccal cell line, while certain triggered the production of reactive oxygen species (Teubl et al. 2015a; Teubl et al. 2015b). Nonetheless, this evaluation remains to be investigated with the food form of TiO_2 for risk assessment purposes given the mixed composition of nano- and submicron-sized particles in commercial E171 batches.

The median turnover of the buccal mucosa is 14 days (Teubl et al. 2015a), implying active stem

cell division to ensure epithelium renewal. Therefore, in the context of oral exposure, it is important to take into account the role of the cell cycle when assessing particle toxicity. To gain insight into the possible toxic effects of food-grade TiO_2 at the mouth level, the translocation of TiO_2 particles from the food additive E171 was first assessed *in vivo* in piglet mouths, for which the histomorphology of the buccal mucosa is comparable to that of humans. Second, we used the human TR146 cell line, either in cycling or noncycling differentiated cells, as a model of the buccal mucosa composed of cells with different proliferation statuses. The kinetic of the cellular permeability to foodborne TiO_2 particles, as well as cytotoxicity, genotoxicity and oxidative stress in TR146 cells exposed to the food additive were evaluated. Due to the wide particle size distributions in food-grade TiO_2 powders, a comparative toxicity study was also performed with two TiO_2 particle models with distinct primary sizes, below and above 100 nm in diameter.

Materials and methods

Chemicals and particle preparation

Food-grade TiO_2 (E171) was purchased as a powder from the website of a French commercial supplier of food coloring agents and was previously characterized as a representative E171 sample in the anatase crystal form that has been placed on the EU market (Guillard et al. 2020). Two other (anatase) TiO_2 test materials with distinct primary particle sizes were used in this study, namely 21 nm TiO_2-NP (Sigma–Aldrich, Saint-Quentin-Fallavier, France) and 115 nm NM-102, referenced to JRCNM10200a by the European Joint Research Center Nanomaterials Repository (JRC, Ispra, Italy). TiO_2 materials were sonicated in ultrapure water (1 mg/ml) placed in an ice bath for 1 min at 40% amplitude (VCX 750-230 V, Sonics Materials) to obtain a stable dispersion of TiO_2 particles for 15 days at 4 °C. Dynamic light scattering (DLS; Zetasizer Nano ZS; Malvern Instruments Ltd.) measurements were performed on each TiO_2 material in ultrapure water (pH = 7.75) and in TR146 cell culture medium (Ham's F12, pH 7.54; Life Technologies, Illkirch, France). Ten microlitres of E171, NM-102 or TiO_2-NP suspensions were diluted in 2 mL of ultrapure water or Ham's F12 medium, and the hydrodynamic diameter (Z-average), polydispersity index and zeta potential were measured. In addition, some E171 samples were prepared without dispersion protocol for *in vivo* experiments with pigs.

Animals and study design for in vivo buccal exposure

Five 4-week-old weaned castrated male piglets (Pic 410) weighing 10–12 kg were obtained from a local swine supplier (Gaec de Calvignac, Saint-Vincent d'Autejac, France). All animal studies were carried out in accordance with the European Guidelines for the Care and Use of Animals for Research Purposes (Directive 2010/63/EU) and validated by the Ethics Committee for Animal Experiments Toxcomethique n° 86 (TOXCOM/121/LGU). Pigs were acclimatized for 1 week in the animal facility of the INRAE Research Center in Food Toxicology (Toxalim, Toulouse, France) and fed *ad libitum* with free access to water. One pig served as a control, being administered water free from the food additive E171, and the other 4 pigs were exposed to TiO_2 (E171) water suspension, dispersed ($n = 2$) or not ($n = 2$) by sonication. During a short restraint operated by an animal technician, a volume of 200 µl of food-grade TiO_2 (E171) water suspension (50 µg/ml) was gently deposited once at T0 in the mouth under the tongue using a syringe equipped with a flexible catheter to avoid any injury in the mouth. The same procedure was repeated at T0 + 1, 2 and 3 h, and animals were euthanized at T0 + 30 min ($n = 2$) or at T0 + 4 h, i.e., one hour after the last sublingual deposit ($n = 3$, including the control pig). During the exposure period, all piglets were allowed to move freely in the barn without access to water or feed to avoid dilution in the mouth. At sacrifice, tissue samples from the buccal cavity under the tongue (buccal floor) as well as the submandibular lymph nodes located underneath the tongue were quickly withdrawn and prepared for TEM analysis.

Buccal tissue preparation for TEM-EDX analysis

Tissue samples from piglets were fixed in 2.5% paraformaldehyde-2.5% glutaraldehyde in 0.1 M cacodylate buffer (pH 7.4) overnight at 4 °C. After

several rinses with cacodylate buffer, the samples were postfixed in 1% OsO_4 (Osmium (VIII) oxide) for 1 h (4 °C) and then rinsed again with cacodylate buffer before being dehydrated using a graded series of ethanol. The sections were impregnated in low viscosity epoxy resin (EMS) under vacuum and then polymerized at 60 °C for 48–72 h. Ultrathin sections (80 nm, Ultracut UCT, Leica) were collected on copper grids and stained with a UAR-EMS (uranyl acetate replacement) solution followed by a 0.4% lead citrate solution. Five to 6 tissue sections from each sample were observed under a JEOL JEM-1400 electron microscope (MeTi facility, Toulouse, France) operated at 200 kV for TEM observations of electron dense particles and analyzed by energy-dispersive X-ray spectroscopy (EDX) on a JEOL 2100 F (Raymond Castaing facility, Toulouse, France) for chemical elemental analysis. Measurements of minimum and maximum Feret diameters were performed from bright-field TEM images by using the image processing open-source software ImageJ (NIH, United States).

Cell culture and TiO_2 treatments

Human TR146 buccal epithelial cells (Sigma–Aldrich) were cultured in Ham's F12 nutrient mix (Life Technologies) supplemented with 10% fetal bovine serum (FBS; Gibco, Life Technologies) and 0.1% penicillin/streptomycin. Cells were maintained at 37 °C in a humidified atmosphere containing 5% CO_2 and subcultured every 2–3 days. To differentiate the TR146 cells, 10 000 cells were seeded in 0.33 cm^2 Transwell inserts (Corning) for 30 days, and the culture medium was changed every 2–3 days. Cells were exposed for 2 h to different concentrations of food-grade TiO_2 (E171) (5, 50 or 100 µg/ml) or to the test materials TiO_2 (NM-102 and TiO_2-NP) in Ham's F12 without FBS and when indicated, washed twice with PBS before being incubated in fresh complete culture medium.

Confocal microscopy, TEM and SIMS imaging on TR146 cells

To study the kinetics of food-grade TiO_2 particle absorption, human epithelial TR146 cells were exposed for 1 h, 2 h, 5 h and 24 h to a 50 µl/ml suspension of TiO_2 (E171) in Ham's F12. Control cells were exposed to Ham's F12 only. Supplemental TR146 cells exposed to E171 for 2 h were rinsed with Ham's F12 before being cultivated for a 5 h wash-out period in the same culture medium free of TiO_2 particles. For confocal microscopy, TR146 cells were fixed in 4% buffered formalin, embedded in paraffin wax, and sectioned to a thickness of five microns. Sections were first incubated with WGA-Alexa 594 for 1 h in the dark and then washed before being mounted with DAPI (4′,6-diamidino-2-phenylindole; Life Technologies, France)-containing ProLong Gold antifade mounting medium for fluorescence microscopy. Tissue sections were viewed under a Leica SP8 confocal microscope with a 40× immersion objective and examined at 488/BP 488–494 nm to detect laser reflection by the metal particles as previously described (Coméra et al. 2020).

For TEM, TR146 cell monolayers were treated as previously described for buccal tissues. Since EDX might not be sensitive enough to allow investigation of the uptake of single NPs in cell preparations, correlative high-resolution imaging and secondary ion mass spectrometry (SIMS) were performed using a customized Zeiss Orion NanoFab helium ion microscope called the 'npSCOPE' instrument (De Castro et al. 2021) developed in the framework of EU HORIZON 2020 project no. 720964. TR146 cells exposed for 24 h to food-grade TiO_2 (E171) were fixed and embedded as for electron microscopy. Unstained 60 nm thick sections were cut, placed on an EM grid and investigated on the npSCOPE. Secondary electron (SE) and scanning transmission ion microscopy (STIM) images were recorded with a He^+ primary beam at 30 keV at a working distance of 7.5 mm. Acquisition conditions were as follows: beam current, 3.4 pA, and dwell time of 5 µs, with an average of 4 frames for the SE images; beam current, 0.1 pA, and dwell time of 600 µs for the STIM images. SIMS was performed with a Ne^+ primary beam at 20 keV, beam current of 8–10 pA and a working distance of 18.7 mm on the same area of interest. Positive mode SIMS was acquired at a magnetic field of 364 mT with a dwell time of 2 ms, while negative SIMS was acquired at a magnetic field of 300 mT with a dwell time of 8 ms.

Cell viability

The AlamarBlue® (Life Technologies) assay was used to evaluate the proliferation and viability of proliferating TR146 cells grown on 96-well plates, or to evaluate the viability of differentiated cells grown on Transwell inserts. For proliferating cells, 2000 cells were seeded per well and incubated for 24 h. The cells were exposed to 25 μM of etoposide as a positive control, or different concentrations (5, 50 or 100 μg/ml) of food-grade TiO_2 (E171) and TiO_2 test materials for 2 h. Cells were then washed twice with PBS and incubated in fresh culture medium for 72 h to allow at least two rounds of cell division for proliferating cells. Viability and proliferation were assessed using the AlamarBlue® assay according to the manufacturer's instructions. The fluorescence was measured at an excitation of 570 nm and emission of 610 nm using a SPARK spectrophotometer. At least three independent experiments were performed.

Transepithelial electrical resistance

The transepithelial electrical resistance (TEER) of differentiated TR146 cells was monitored using a Millicell-ERS voltohmmeter (Millipore, Saint-Quentin-en-Yvelines, France). Cells were treated with food-grade TiO_2 or the TiO_2 test materials for 2 h, washed twice with PBS and incubated in fresh culture medium. The TEER was measured immediately and then measured again at the indicated times for 48 h. The TEER values were normalized to that of the untreated condition. At least three independent experiments were performed.

Immunofluorescence and oxidative stress analyses

Proliferating TR146 cells were grown on glass coverslips. After at least 24 h of culture, cells were exposed to 50 μM of etoposide or menadione as positive controls for genotoxic and oxidative stresses, respectively, or to food-grade TiO_2 (E171) and the TiO_2 test materials for the indicated times and concentrations before being fixed with 4% paraformaldehyde. For the oxidative stress assays, 30 minutes before fixation, 5 μM CellRox® Green Reagent (Life Technologies) was added to the cells for incubation at 37 °C in the dark. For immunofluorescence assays, cells were permeabilized with 0.5% Triton X-100, blocked with 3% BSA and 0.05% IGEPAL, and stained with primary antibodies (γH2AX antibody (05–636), Sigma–Aldrich; 53BP1 antibody (NB100-304), Bio-Techne, Noyal-Châtillon-sur-Seiche, France) overnight at 4° C in blocking solution (all solutions were prepared in PBS). Cells were washed three times with PBS 0.05% IGEPAL and incubated with the secondary antibodies (Alexa Fluor 488 or 594 goat anti-mouse or Alexa Fluor 594 goat anti-rabbit; Life Technologies) for 1 h at room temperature. DNA was stained with 30 nM of DAPI. Coverslips or membranes cut out of the Transwell inserts were mounted onto slides with PBS-glycerol (90%) containing 1 mg/ml paraphenylenediamine and observed at 20× magnification with a Nikon 50i fluorescence microscope equipped with a Luca S camera. Upon oxidation, CellRox® Green Reagent exhibits strong fluorescence and binds to DNA. Therefore, as for γH2AX, the signal intensity of CellRox® Reagent was automatically determined by an ImageJ macro in each nucleus. The γH2AX or CellRox® Reagent signal intensity of the whole cell population was averaged for each condition, and these results were normalized to 1 for the untreated samples. For each experiment, 200–250 cells were counted, and at least three independent experiments were performed.

Comet assay

Proliferating TR146 cells were exposed to 50 μM of etoposide as a positive control or to food-grade TiO_2 (E171) and the two TiO_2 test materials for the indicated times at the indicated concentrations. The comet assay was performed under alkaline conditions using a Comet SCGE assay kit (Enzo Life Sciences, Villeurbanne, France) according to the manufacturer's instructions. Briefly, 800 cells embedded in low-melting agarose were spread in each sample area of the comet slide. Electrophoresis was performed in alkaline solution (0.3 N NaOH, 1 mM EDTA) at 4° C for 30 min at 35 V in a large electrophoresis tank (35 cm between electrodes). After staining with CYGREEN® Nucleic Acid Dye, slides were observed at 20× magnification using a Nikon 50i fluorescence microscope equipped with a Luca S camera. At least 60 cells were analyzed per sample using OpenComet

software. At least three independent experiments were performed.

Micronucleus assay

Proliferating TR146 cells were grown on glass coverslips. After at least 24 h of culture, cells were exposed to 50 μM of etoposide as positive control or to food-grade TiO_2 (E171) and the TiO_2 test materials for 2 hours before to be released in fresh medium for 22 hours. Cells were then fixed with 4% paraformaldehyde and treated as for immunofluorescence analyzes. Cells were observed at 40× magnification with a Nikon 50i fluorescence microscope equipped with a Luca S camera. The frequency of micronucleated cells was scored on at least 100 cells per sample. At least three independent experiments were performed.

Statistical analysis

The results are expressed as the mean ± SD of at least 3 independent experiments. Statistical analysis was performed with Prism 8 software (GraphPad Software Inc., San Diego, CA, USA). Differential effects were analyzed by one-way or two-way analysis of variance (ANOVA) followed by the appropriate post hoc test (Dunnett or Sidak). A p value $<$ 0.05 was considered significant ($^{*}p < 0.05$; $^{**}p < 0.01$; $^{***}p < 0.001$; $^{****}p < 0.0001$).

Results

Physico-chemical characteristics of the TiO_2 particles

The commercial E171 batch of food-grade TiO_2 used herein was previously characterized for its particle size distribution by SEM analysis. It was shown that 55% of the NPs by number were 20 to 440 nm for a mean size of 105 ± 45 nm (Guillard et al. 2020). DLS was carried out to determine the hydrodynamic diameter and zeta potential in ultrapure water, and the sample was also analyzed by BET for specific surface area (Guillard et al. 2020). Correlative secondary electron and SIMS imaging with the npSCOPE recently confirmed the SEM data, also providing chemical information with $<$ 20 nm resolution (De Castro et al. 2021). Using TEM imaging, the TiO_2 particles from the E171 food additive dispersed into ultrapure water were mostly recovered as isolated particles mixed with small aggregates and agglomerates of particles of various sizes (Figure 1). Additional DLS analyses of the food-grade TiO_2 particles in the present study showed a slight increase in hydrodynamic diameter after resuspension in Ham's F12/TR146 cell culture medium compared to that in water suspension (Table 1). Similar observations were found for NM-102, while the TiO_2-NP material exhibited a larger agglomeration state in the culture medium compared to the water suspension (Table 1).

In vivo translocation of food-grade TiO_2 through pig oral mucosa

The concentration chosen for *in vivo* buccal exposure to pigs (50 μg/ml) was considered realistic for human exposure given the current estimate of TiO_2 concentrations for example from chewing gum coated with E171 (range 0.35–15.25 mg TiO_2/gum) (Fiordaliso et al. 2018), local loading of TiO_2 in the mouth during chewing (Supplementary Figure S1) and mean oral volumes of saliva of 1 and 0.5 ml in adults and children, respectively (Lagerlöf and Dawes 1984; Watanabe et al. 2021). In buccal tissues, TEM-EDX was used to investigate the transmucosal passage of TiO_2 particles from the food additive deposited under the tongue once every hour for 3 h. Translocated particles were recovered deep into the buccal tissues in all E171-exposed pigs ($n = 4$), as illustrated in Figure 2. Indeed, 30 minutes after the first sublingual deposit of E171, the TEM observations clearly showed the presence of electron-dense particles that had translocated into the mucosa (Figure 2(A)). As shown in Figure 2(A), EDX analysis clearly revealed the presence of titanium (Ti) on a particle of 104 nm (smaller diameter) recovered from the buccal floor, while no Ti particles was observed in the submandibular lymph nodes at 30 min.

At 4 h (i.e., 1 h after the last E171 deposit), electron-dense particles were observed in the mucosa of buccal floor (Figure 2(B1,C1)) as well as in the lumen of blood capillaries (Supplementary Figure S2). TEM-EDX analysis of 6 tissue sections sampled from the buccal floor showed that most particles recovered in the mucosa (i.e., 15 of 17) were Ti-positive (Figure 2(B2,C2), and Table 2). They

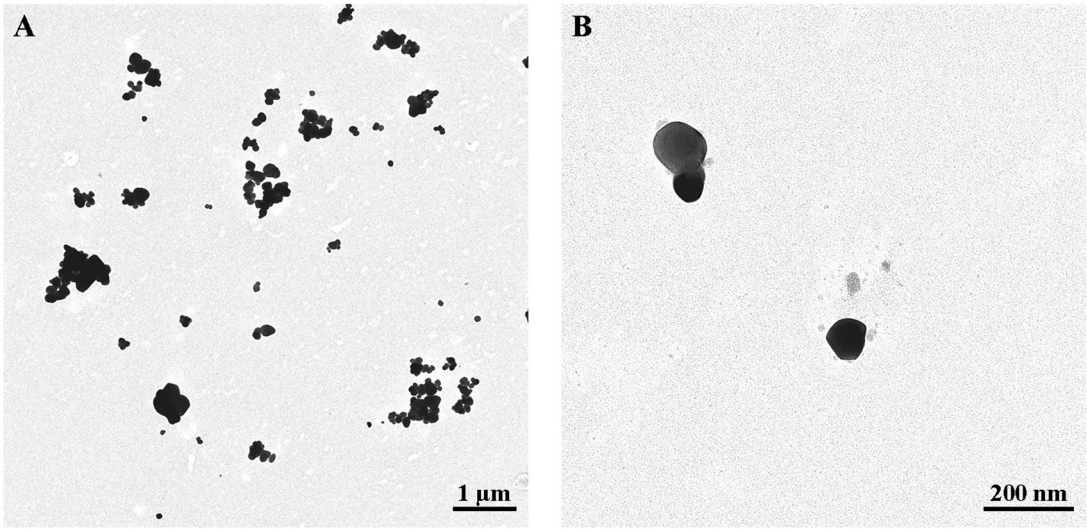

Figure 1. TEM images of food-grade TiO_2 (E171) particles. E171 powder after dispersion in ultrapure water at low (A) and high (B) magnification showing morphology of isolated and aggregated TiO_2 particles.

Table 1. TiO_2 sample characterization by DLS.

	Ultrapure water (pH = 7.75)			Ham's F12 medium (pH = 7.54)		
TiO_2 sample	Zeta potential (mV)	H.diam. (nm)	PdI	Zeta potential (mV)	H.diam. (nm)	PdI
E171	−32.1 ± 0.79	297.9 ± 5.1	0.21	−8.97 ± 0.54	318.7 ± 14.9	0.40
NM-102	−34.3 ± 0.66	301.6 ± 0.4	0.17	−8.19 ± 0.59	337.0 ± 20.1	0.35
TiO_2-NPs	−11.1 ± 2.44	173.9 ± 1.7	0.16	−8.99 ± 1.96	226.4 ± 3.1	0.39

All data are presented as the mean ± SD. H. diam.: hydrodynamic diameter; PdI : polydispersity index.

appeared as isolated particles ($n = 6$) (Figure 2(B1)) or as small aggregates ($n = 9$), the later being composed of 2 to 11 particles fused together (see Figure 2(C1)). Analysis of minimum Feret diameters showed isolated particles ranging from 72 to 199 nm, and aggregates from 117 to 392 nm (Table 2), and up to 550 nm in maximum Feret diameter for aggregates (Table 2). In addition, at 4 h, Ti was also found in isolated particles ($n = 1$) and aggregates ($n = 7$) recovered from tissue sections sampled from the submandibular lymph nodes located underneath the tongue (Figure 2(D)), and were similar in size range to those observed in the buccal floor (Table 2). In the control pig exposed to water only, no Ti signal was observed over 9 electron-dense objects found in the buccal mucosa, while only one Ti particle of 10 was recovered in the submandibular lymph nodes, showing irregular shape and mix composition with Si and Al elements (Supplementary Figure S3) not observed with E171 buccal exposure.

When pigs were treated for 4 h with the food additive E171 without sonication (i.e., not dispersed), TEM-EDX analysis also showed Ti-positive particles in the buccal floor (7 particles/aggregates of 26 analyzed) and in the submandibular lymph nodes (3 of 17) (Supplementary Figure S4 and Supplementary Table S1). This showed transmucosal passage of food-grade TiO_2 as raw powder in water suspension, where translocated particles and aggregates exhibited sizes similar to those recovered using dispersed E171 preparation as described above (Table 2 and Supplementary Table S1).

Kinetic of TR146 cell permeability to TiO_2 food additive

To assess the absorption kinetics of food-grade TiO_2 particles by human oral epithelial cells, TR146 cells were first observed by confocal microscopy after 1, 2 and 5 h of exposure to the food additive E171 (50 µg/ml) or after 2 h of exposure followed by 5 h of incubation in fresh culture medium free of E171 (i.e., wash-out). As shown in Figure 3, the laser-diffracting TiO_2 particles appeared as a bright green signal upon more or less agglomerated particles once absorbed by the cells (Figure 3(A–D)), as previously described (Coméra et al. 2020; Guillard et al. 2020). In 1 h-exposed cells, some laser-diffracting particles were recovered in the cytoplasm, some of

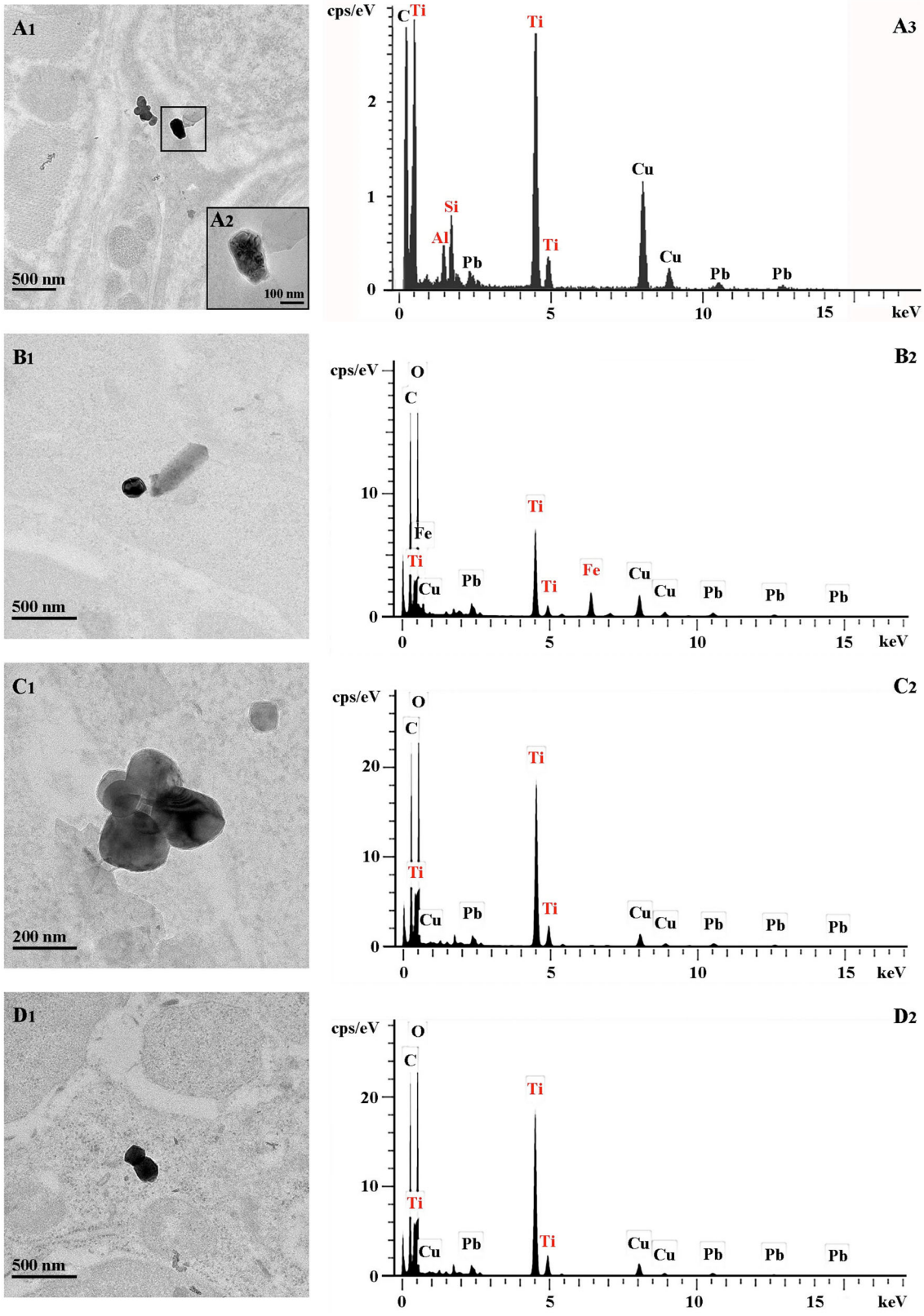

Figure 2. TEM imaging and EDX analysis of ultrathin sections of the buccal mucosa and submandibular lymph nodes from pigs exposed to food-grade TiO_2 particles (E171). (A) TEM images (A1-2) and the corresponding EDX analysis for elemental analysis (A3) of the Ti(O_2) particles translocated into the buccal floor 30 min after a single E171 sublingual deposit. Note in the EDX spectrum (A3) additional Al and Si signals as main elements over an adjacent particulate deposit appearing as a chapelet (A1). Copper (Cu) and lead (Pb) are from the sample grid and lead citrate staining, respectively. (B,C) TEM images (B1-C1) and the corresponding EDX spectra (B2-C2) of the Ti(O_2) particles in the buccal mucosa at 4 h, i.e., one hour after the last E171 sublingual deposit. Note in (B1) the presence of an elongated Fe particle in the same microscopic field. (D) TEM image (D1) and the corresponding EDX analysis (D2) of the Ti(O_2) particles translocated into a submandibular lymph node at the same time point.

Table 2. TiO_2 particles in pig buccal mucosa and submandibular lymph nodes after repeated sublingual deposition for 4 h of E171 suspension dispersed in water.

Tissue sample	Number of analyzed electron-dense particles	Ti-positive particles ($D_{MinFeret}/D_{MaxFeret}$ ±SD in nm)	
		isolated	aggregates
Buccal floor	17	6 (143 ± 49/191 ± 88)	9 (257 ± 99/393 ± 116)
Submandibular lymph nodes	14	1 (129/140)	7 (257 ± 97/390 ± 120)

$D_{MinFeret}/D_{MaxFeret}$: minimum and maximum Feret Diameters.

which were in close contact with the nucleus (Figure 3(A)). The number of laser-diffracting particles progressively increased after 2 and 5 h of treatment (Figure 3(B,C)). No laser-reflective particulate matter was observed in the nucleus regardless of the time point. In cells exposed to the food additive for 2 h followed by 5 h of wash-out, large agglomerates of laser-diffracting particles were still present in the cytoplasm (Figure 3(D)), suggesting that TiO_2 could penetrate the buccal epithelium and that these particles would not be cleared from the cells even several hours after the end of exposure *in vitro*.

To achieve better resolution, a second set of experiments was carried out with TEM observations, which confirmed the large capacity of the TiO_2 particles to permeate TR146 cells over time. Electron-dense (TiO_2) particles were isolated or recovered as small aggregates and then larger agglomerates of submicron-sized particles mixed with NPs into the cytoplasm (Figure 3(E)). Again, absorbed TiO_2 were still observed 2 h after E171 treatment following wash-out (Figure 3(F)).

Cell areas containing electron-dense particles were further investigated by npSCOPE analyses combining SE, STIM and SIMS imaging for unprecedented TiO_2 identification within the cell matrix. As illustrated in Figure 4, single NPs as well as small and large clusters of electron-dense TiO_2 were found embedded in the cytoplasm of TR146 cells after 24 h of treatment with the food additive E171.

Comparative cytotoxicity of the TiO_2 test materials in human buccal cells

To gain insight into the cytotoxic effects of food-grade TiO_2 compared with the two TiO_2 standards with different nominal sizes (NM-102 and TiO_2-NPs: 115 and 21 nm, respectively), proliferating or differentiated TR146 cells were exposed to different TiO_2 concentrations (5, 50, 100 µg/ml) for 2 h. The TR146 cells were then allowed to recover in fresh culture medium for 72 h before cell viability assessment, allowing at leat two rounds of cell division in proliferating cells. In proliferating cells, the DNA damaging agent etoposide (used as positive control) and the three tested TiO_2 samples induced a significant cytotoxic activity at all tested concentrations compared to nontreated cells, except with 5 µg/ml for E171, with a dose-response tendency (Figure 5(A)). In contrast, after cell differentiation, no viability drop was observed in any tested condition (Figure 5(A)). This suggests that etoposide and TiO_2 particles may not directly affect cell viability but rather impede cell proliferation.

In addition, the TEER of differentiated TR146 cells was measured after 2 h of exposure to each TiO_2 sample to assess their respective impacts on epithelial integrity. Regardless of the time point tested during the 48 h after treatment, no alterations were detected at any dose, suggesting that epithelial barrier permeability and monolayer integrity were not affected regardless of the TiO_2 product or particle size (Figure 5(B)). Taken together, these data indicate that the epithelium formed by TR146 cells is not noticeably altered by exposure to foodborne TiO_2 but that cycling cells could be sensitized.

Comparative genotoxicity of the TiO_2 test materials in human buccal cells

Next, we assessed the genotoxic potential of food-grade TiO_2 (E171) and standard TiO_2 products on buccal cells by immunofluorescent analyses using antibodies directed against γH2AX and 53BP1, two well-established DNA damage biomarkers (Vignard, Mirey, and Salles 2013). Proliferating or differentiated TR146 cells were exposed for 2 h to the three different TiO_2 materials at 5, 50 or 100 µg/ml. We first analyzed the phosphorylation of H2AX at

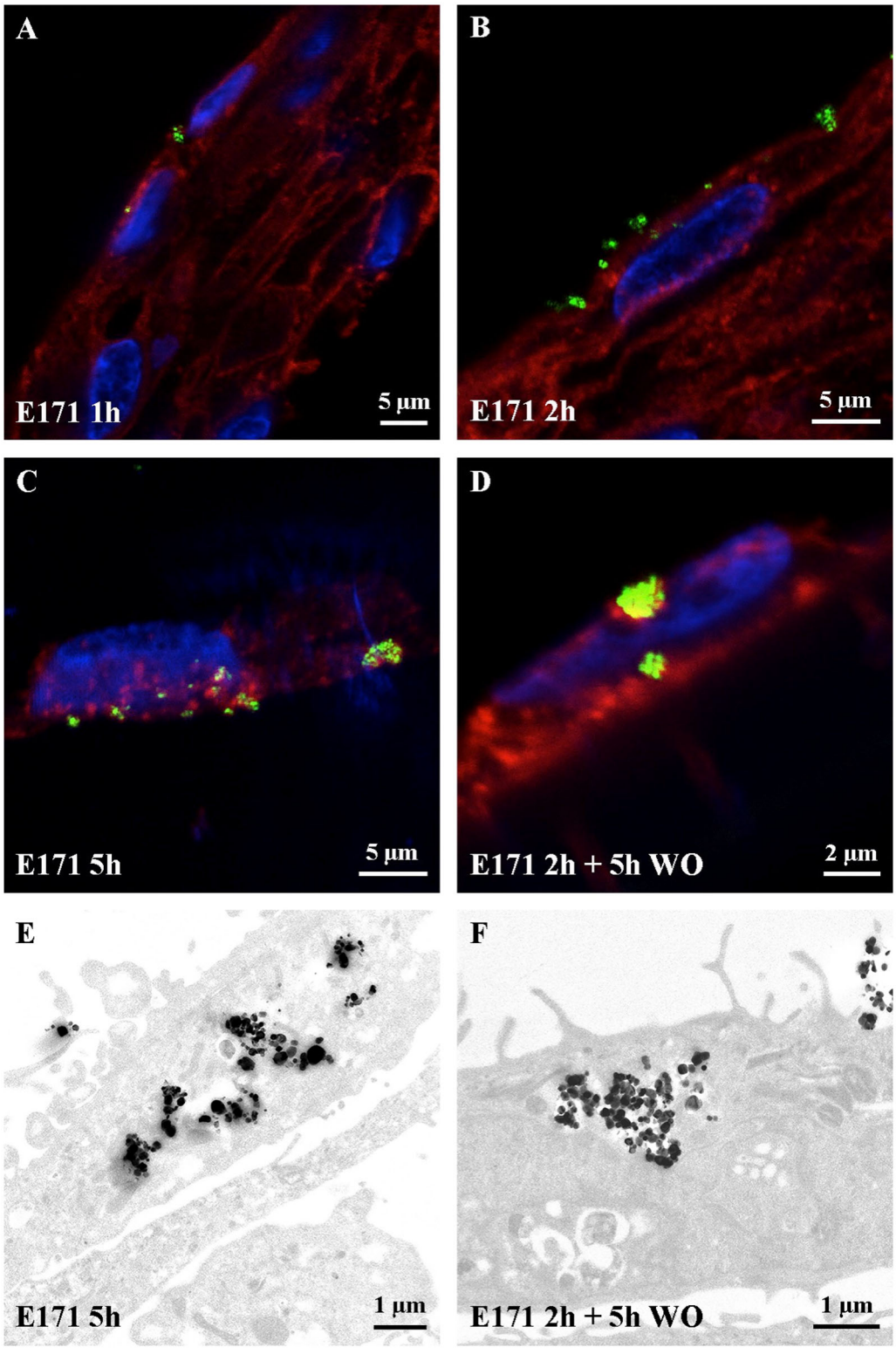

Figure 3. Absorption kinetics of buccal TR146 cells exposed to food-grade TiO_2 (E171) particles. (A-D) Confocal images of TR146 cell sections treated with 50 µg/ml E171 for 1 h, 2 h and 5 h, or 2 h plus a wash-out (WO) of 5 h. The laser-reflecting (metal) particles appear green, the WGA-labelled glycoproteins appear red, and cell nuclei appear blue. (E-F) TEM images of TR146 cell sections treated with 50 µg/ml E171 for 5 h (E) and 2 h followed by a 5 h wash-out (F).

Ser139 (referred to as γH2AX), which occurs at DNA double-strand breaks. While only a few cells presented a γH2AX signal in the control, cells exposed to E171 or NM-102 accumulated γH2AX foci (Figure 6(A)). In contrast, the pure nanopowder of TiO_2-NPs (21 nm) did not increase γH2AX staining (Figure

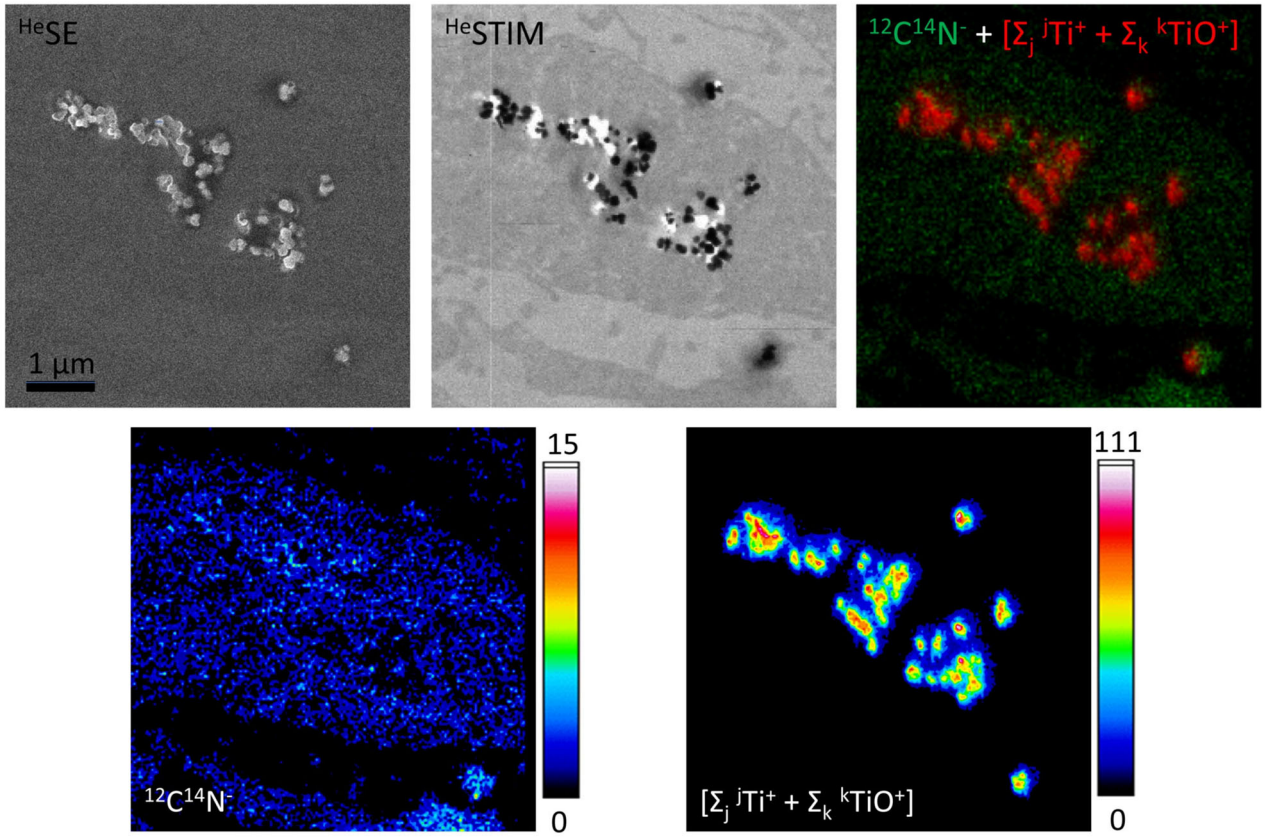

Figure 4. Correlative secondary electron (SE) imaging, scanning transmission ion microscopy (STIM) and secondary ion mass spectrometric (SIMS) elemental mapping of ultrathin sections of buccal TR146 cells exposed to food-grade TiO_2 (E171) particles for 24 hours. In contrast to the TEM images presented in figure 2, SE imaging obtained with a helium ion microscope (here, npSCOPE) reveals predominantly topographical information. The thin sections therefore show only limited contrast of the cell structures and the nanoparticles are easily recognized. For TEM-like imaging, the STIM detector attached to the npSCOPE prototype device allows investigation of the transmitted beam information and highlights the NP in relation to the cellular ultrastructure. The image shows the engulfment of electron-dense particles into the cell cytoplasm. The SIMS image obtained on the same area highlights cellular information when considering the $^{12}C^{14}N$ cluster ion and clearly identifies individual TiO_2 nanoparticles and clusters (lateral resolution down to a particle size of 15 nm). The integrated Ti "Σ"-map represents the signals obtained by summing the peaks of all Ti isotopes and all TiO cluster peaks.

6(A)). We then observed the localization of 53BP1, which is a diffuse nuclear protein that displays a singular localization pattern as large nuclear speckles in unchallenged G1 cells, named 53BP1 nuclear bodies (Fernandez-Vidal, Vignard, and Mirey 2017). These structures represent the major staining found in the control or after exposure to TiO_2-NPs with a nominal size of 21 nm (Figure 6(A)). However, in the presence of DNA double-strand breaks, 53BP1 is recruited to the damaged site and forms foci. Interestingly, food-grade E171 and NM-102 induced 53BP1 foci formation in a subset of TR146 cells, mainly colocalizing with the γH2AX signal (Figure 6(A)). This staining was observed in proliferating as well as in differentiated cells. Hence, these data showed that food-grade and NM-102 TiO_2 but not TiO_2-NPs activate the DNA damage biomarkers γH2AX and 53BP1 after 2 h of treatment, strongly supporting the formation of DNA double-strand breaks.

To confirm the genotoxic potential of E171, we performed an alkaline comet assay in proliferating cells, to detect DNA strand breaks and alkali-labile sites (that induce DNA relaxation under alkaline conditions) (Collins et al. 2023). Under our conditions, etoposide, E171 and NM-102 significantly increased the amount of DNA strand breaks compared to untreated cells, as revealed by an increase in the % tail DNA, whereas no difference was observed after treatment with TiO_2-NPs (Supplementary Figure S5). Taken together, these observations indicated that exposure to E171 or NM-102 induced the formation of DNA strand

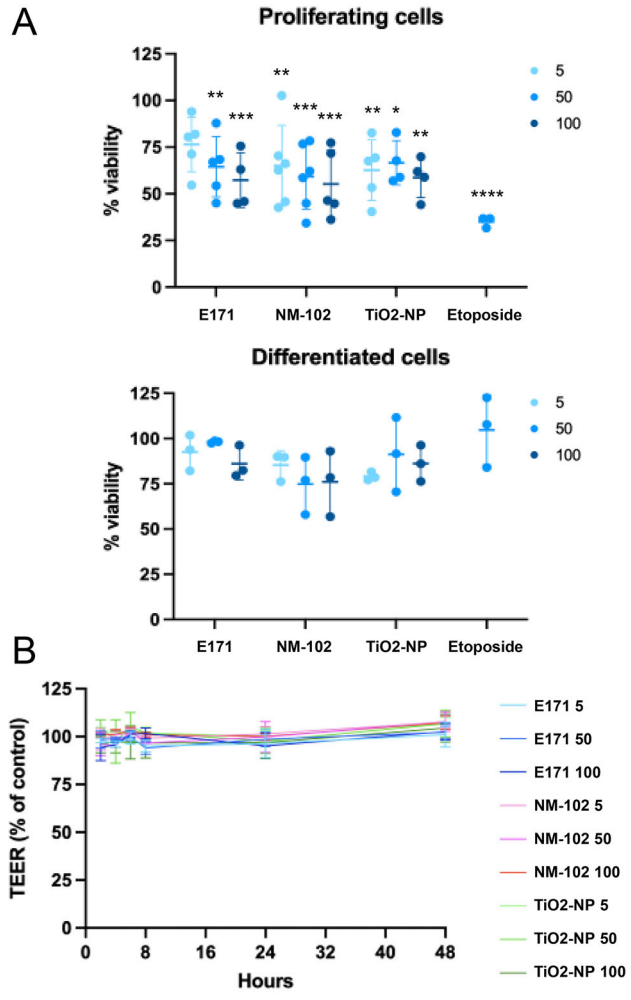

Figure 5. Cytotoxicity of the TiO_2 particles in TR146 cells. Proliferating or differentiated TR146 cells were exposed to 25 μM of etoposide or different concentrations (5, 50 or 100 μg/ml) of E171, NM-102 or TiO_2-NPs. (A) Cell viability was assessed using the AlamarBlue® assay. The graphs represent the viability normalized to that of untreated cells. The results are presented as the mean ± SD of at least three independent experiments. Statistics were calculated by two-way ANOVA followed by Dunnett's multiple comparison test. (B) The TEER was determined in differentiated TR146 cells at different time points after exposure to the TiO_2 materials. The results are presented as the mean ± SD of three independent experiments.

breaks that were signaled by the DNA damage response factors γH2AX and 53BP1 in TR146 cells.

We next assessed the level of DNA damage in TR146 cells at two different timing after exposure to the TiO_2 samples through γH2AX signal quantification. A dose-dependent increase in γH2AX staining was observed after 2 h of exposure to both E171 and NM-102 in proliferating cells (Figure 6(B)), to a lesser extent compared to the positive control etoposide. In differientated cells exposed under the same conditions, a significant increase in the γH2AX level was also detected with E171 and NM-102, but only at a concentration of 100 μg/ml (Supplementary Figure S6). When proliferating TR146 cells were allowed to recover and placed in fresh medium for 22 h, an approximately two-fold decrease in γH2AX signal was observed for etoposide, supporting that some of the DNA lesions were repaired after the recovery period (Figure 6(C)). Proliferating TR146 cells exposed to 100 μg/ml of E171 did no longer exhibit significant difference in γH2AX signal compared to untreated cells after the 22 h recovery time, highlighting the repair of at least part of the DNA damage. However, the fold increase in γH2AX signal was still significant for 50 μg/ml of E171 and for 50 μg/ml or 100 μg/ml of NM-102, showing that some DNA lesions were still present (Figure 6(C)). On the contrary, the γH2AX signals in the differentiated cells exposed to E171, NM-102 and etoposide returned to basal levels after the recovery time (Supplementary Figure S6). In the TiO_2-NP model, the γH2AX signal remained at the same level as the control under all tested conditions (Figure 6(B,C) and Supplementary Figure S6). In conclusion, TR146 cells exposed to food-grade (E171) TiO_2 or NM-102 generated DNA damage, some of which lingered in cycling cells after a period of recovery, suggesting that cell proliferation aggravates the genotoxic activity induced by TiO_2.

Finally, we asked wether E171 could impact the genomic stability of TR146 cells treated as in Figure 6(C), by performing a micronucleus assay. Under our experimental conditions, no clear difference was observed between untreated cells and cells exposed to the different TiO_2 samples, whereas the positive control etoposide induced a significant increase of cells with micronuclei (Supplementary Figure S7).

E171-induced oxidative stress in human buccal cells

As many previous studies have reported that TiO_2-related genotoxicity mainly resulted from oxidative stress, we monitored the production of reactive oxygen species (ROS) using the fluorogenic probe CellROX® Green Reagent in proliferating TR146 cells exposed to the food additive E171 and two TiO_2 test materials for 2 h. CellROX® Green Reagent

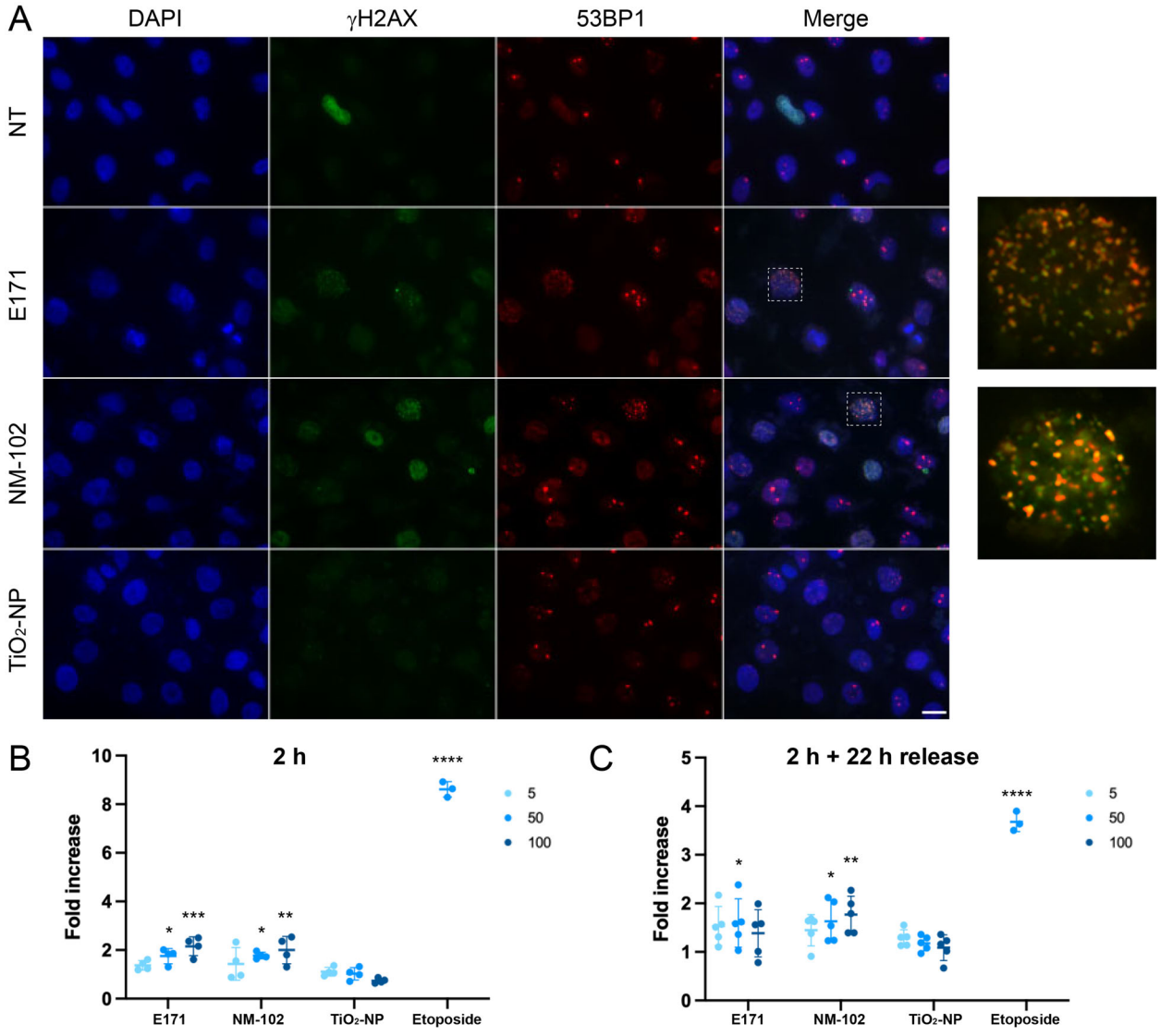

Figure 6. Genotoxicity of the TiO_2 particles in TR146 cells. (A) TR146 cells were left untreated (NT) or exposed to 50 μg/ml E171, NM-102 or TiO_2-NPs for 2 h and analyzed by immunofluorescence microscopy with antibodies against γH2AX and 53BP1. The images on the right represent magnification of the cells delineated by squares with white dotted lines (γH2AX and 53BP1 signals). (B, C) Proliferating TR146 cells were treated with 50 μM of etoposide or different concentrations of TiO_2 (5, 50 or 100 μg/ml), and the γH2AX signal was quantified immediately (B) or after 22 h of recovery in fresh culture medium (C). The results are presented as the mean ± SD of at least three independent experiments. Statistics were calculated by one-way ANOVA followed by Dunnett's multiple comparison test.

emits green fluorescence upon oxidation by ROS and subsequently binds to DNA. Compared to untreated cells and TiO_2-NP treatments, cells exposed to the food-grade E171 and NM-102 exhibited green nuclear fluorescence after incubation with CellROX Green Reagent (Figure 7(A)), indicative of ROS production. Of note, these signals were slight compared to the positive control menadione. With the food additive E171 and contrary to the results with NM-102 or menadione, quantification did not allow us to conclude that there was significant difference compared to untreated cells (Figure 7(B)). However, when the cells were allowed to recover in fresh culture medium for 22 h, CellROX® Green signal persisted and showed a significant increase after exposure to both E171 and NM-102 at 100 μg/ml (Figure 7(C)). Therefore, a short-term exposure to food-grade TiO_2 can induce weak ROS production in TR146 cells, which is maintained for at least 22 h following cell absorption.

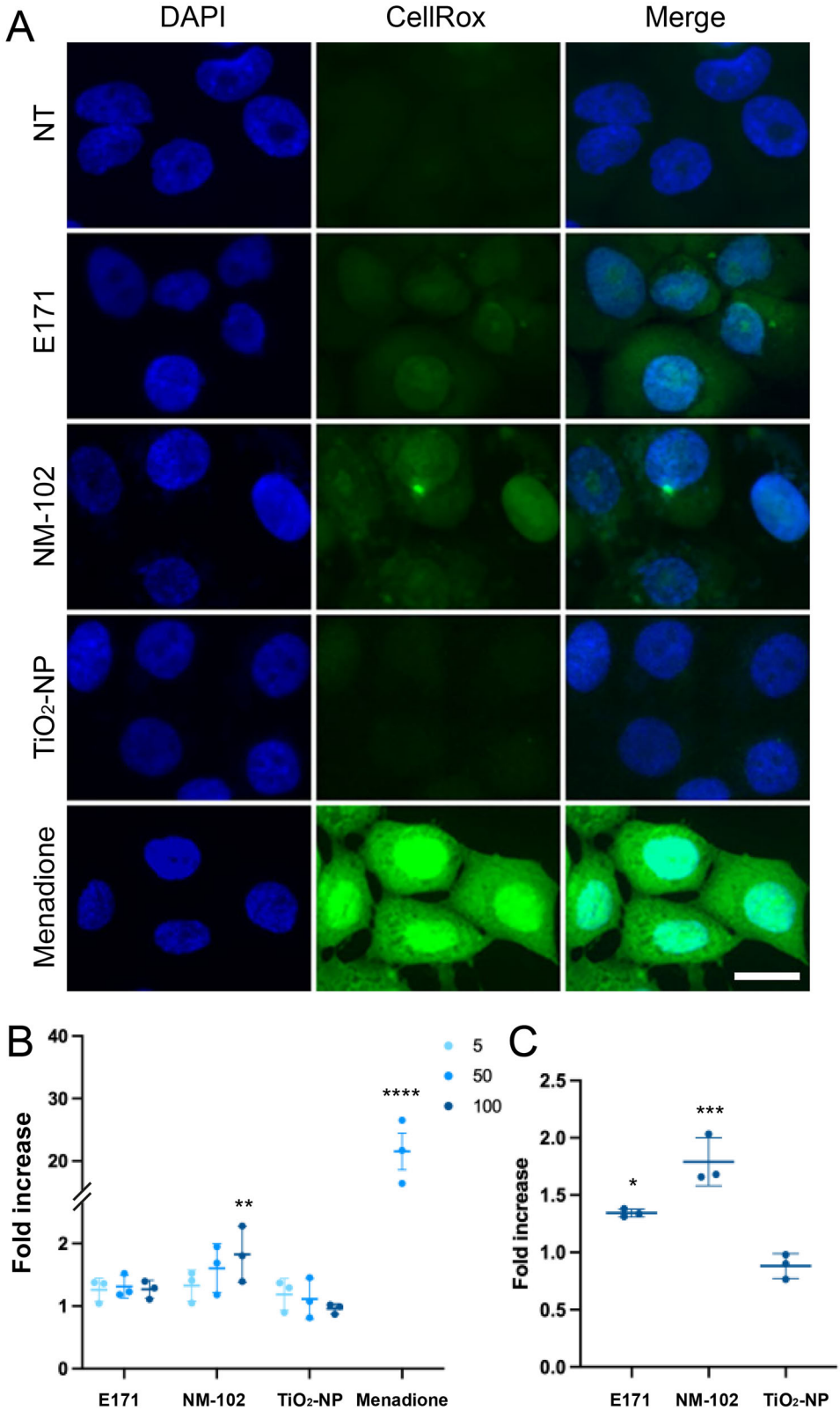

Figure 7. Oxidative stress induced by TiO_2 particles in TR146 cells. (A, B) TR146 cells were left untreated (NT) or exposed to 50 μM of menadione or different concentrations (5, 50 or 100 μg/ml) of E171, NM-102 or TiO_2-NPs for 2 h, and the presence of reactive oxygen species was quantified by using CellROX® Green Reagent. Representative images (A) and quantification (B) are shown. The results are presented as the mean ± SD of three independent experiments. Statistics were calculated by one-way ANOVA followed by Dunnett's multiple comparison test. (C) TR146 cells were treated as in A and B with 100 μg/ml TiO_2 agents and analyzed after 22 h of recovery in fresh culture medium. The results are presented as the mean ± SD of three independent experiments. Statistics were calculated by one-way ANOVA followed by Dunnett's multiple comparison test.

Discussion

Due to the worldwide usage of TiO_2 as coloring agent in common foodstuffs, including drinks and ice cream, or in pharmaceuticals as a coating agent, these different TiO_2-containing products are viewed as the main source of body contamination by TiO_2-NPs in humans. However, in the context of oral route, the contribution of the buccal mucosa for TiO_2 uptake remains poorly documented. The buccal epithelium represents the first surface that is exposed to foodborne xenobiotics. Even though the potential for compound absorption is high in this tissue, as reported for various drug delivery systems including immediate release tablets (Madhav et al. 2009), the buccal epithelium is still not taken into account for risk assessments of the food additive TiO_2 containing a nanosized particle fraction. In the present study, using an *in vitro* model of the human oral epithelium, we report that buccal cells are highly permeable to the TiO_2 particles present in a commercial food-grade (E171) sample, including its NP fraction. To ensure that such passage occurs *in vivo*, we further show that TiO_2 particles rapidly cross the oral epithelium in piglets and are recovered deeper in the buccal mucosa and submandibular lymph nodes after repeated sublingual deposition. In human TR146 cells, we report cytotoxicity and genotoxicity in proliferating cells exposed to E171. The genotoxic effects were still observed after cell differentiation, suggesting the long-lasting impact of food-grade TiO_2 on the human oral epithelium, which should be considered for risk assessment purposes with this food additive.

Using fresh *ex vivo* porcine buccal mucosa as a model for the permeation assessment of NPs into the mouth, a previous study using non-food TiO_2-NP models of various sizes (namely JRC NM100, NM101 and NM105) highlighted the ability of nanosized TiO_2 particles to penetrate the oral cavity tissues (Teubl et al. 2015a). The authors concluded that smaller the NPs (i.e., NM101, 28 nm in Feret minimum diameter) exhibit less depth translocation and remained in the cytoplasm of the surface epithelial cells. In contrast, larger TiO_2 particles, such as NM 100 (displaying two fractions of 34 to 148 nm) or NM 105 (36 nm), also penetrated, but their penetration was deeper into the porcine mucosa. This is in line with our *in vivo* observation in piglets that isolated TiO_2 particles of the E171 additive ranging from 70 to 200 nm in diameter were recovered deep in the oral mucosa. Interestingly, this corresponds to the larger fraction of particle size of food-grade TiO_2 in the E171 batch used in the current study, as previously characterized for primary size distribution by number (Guillard et al. 2020). Notably, such particle translocation occurred rapidly, since it was observed from thirty minutes after a single deposition of the E171 water suspension under the tongue. In addition, *in vitro*, using a human oral cell line (H376) exposed to carboxyl polystyrene particles with sizes of 20 and 200 nm, permeation of the buccal epithelium was reported to be dependent not only on primary particle size but also on agglomeration state in the culture medium (Roblegg et al. 2012). As more agglomeration occured outside the cells, less penetration was observed into the buccal cells. Based on these studies, a similar conclusion can be drawn from the present kinetic study focused on food-grade TiO_2. Although it was restricted to the sole epithelial layer with the TR146 cell line, this *in vitro* model is viewed as able to mimic the human buccal epithelium (Nielsen and Rassing 2000). Both nanosized and submicron-sized TiO_2 particles were found to be endocytosed as single particles or small aggregates, while the very large agglomerates that had previously formed in culture medium remained in contact with the external surface of the epithelial cells without apparent translocation under such large forms (not shown). The current evaluation of the absorption rate using confocal imaging at different time points completed with TEM and SIMS imaging data for high-resolution and elemental characterization, strengthens the idea that food-grade TiO_2 particles enter the cells as isolated particles or as very small aggregates regardless of their nominal size (i.e., NPs or submicron-sized). Such translocation started within 1 h, showing the passage of the particles that progressively accumulated over time into the cells, until 24 h of exposure in the current study, altogether showing high absorption capabilities for oral epithelium. Of note, the time-dependent agglomeration of TiO_2 particles in TR146 cells in our study is due to cell culture grown on filters as a monolayer, which prevented further passage of the particles beyond

the cells and resulted in progressive accumulation in the cytoplasm. The kinetics for particle absorption determined that human buccal epithelial cells are highly permeable to TiO_2, in contrast to the low absorption rate by Caco-2 enterocytes used as an intestinal *in vitro* model (Brun et al. 2014). In buccal cells, no translocation to the nucleus was observed in the current study, which is in line with observations by Teubl et al. Teubl et al. (2015a) using different TiO_2 NP models from the JRC. The rapid absorption of food-grade TiO_2 NPs by the oral epithelium is also in accordance with their study showing that the NPs were internalized within 10 min following exposure. *In vivo* and as stated above, because the size range for isolated particles recovered in the pig oral mucosa corresponded to particle distribution in the commercial E171 powder (Guillard et al. 2020), we concluded the E171 sample the only source for orotransmucosal passage of TiO_2, and that most particles that composed a common commercial batch of E171 can be absorbed in the mouth. Of note, since TiO_2 particles were also found in the pig buccal mucosa with a E171 suspension without sonication for particle dispersion, it is concluded that an orotransmucosal passage also occurs from the food additive in its raw commercial form. These *in vivo* data using pig mouth for which the histomorphology of the buccal mucosa is comparable to that of humans confirmed that the food-grade TiO_2 particles rapidly pass through the surface epithelium in the mouth to reach mucosa underneath, thereby becoming systematically available. Because we herein report aggregate sizes up to 550 nm in the oral mucosa, this suggested that the buccal epithelium is unable to block the passage of such large inorganic structures *in vivo*. An unexpected result was the presence of TiO_2 particles of similar sizes and forms in the submandibular lymph nodes of exposed pigs, and whatever the initial preparation for E171 suspension (i.e., dispersed or not). As key players in the local immune system, lymph nodes act as the first line of defence against harmful agents from the oro pharyngeal region by filtering the lymphatic fluid of unwanted debris and antigens. Studies focused on dental prostheses and titanium implants have already reported Ti particle deposition in the submandibular lymph nodes due to microscopic disintegration of biomedical devices (Onodera, Ooya, and Kawamura 1993; Weingart et al. 1994; Ng et al. 2021). The current study highlights that food-grade TiO_2 particles are also drained by the lymphatic fluid from the oral cavity and then transported to the local lymph nodes. However based solely on this, it is not possible to reach any conclusion regarding an inflammatory risk that requires chronic exposure to be evaluated. Finally, to conclude our kinetic study, and based on recent evaluations of TiO_2 intake from chewing gum that have estimated human exposure ranging from 0.1–84 billion TiO_2 NPs/kg bw/d (Fiordaliso et al. 2018), our study highlights the oral epithelium as a route for the direct systemic passage of food-grade TiO_2 (E171) NPs which has not been taken into account in previous toxicokinetic studies and human risk assessment.

We then explored the potential toxicity impacts of food-grade TiO_2 exposure in the mouth. Human TR146 cells were exposed to E171 for 2 h to ensure particle uptake without accumulation in the cells, as noted above. Experiments were conducted over a range of doses (i.e., 5, 50, 100 μg/ml) for a realistic scenario of the buccal epithelium coming in contact with the food-grade pigment. We first reported cytotoxic activity of E171 only in proliferating cells. In contrast, no defects were observed in TR146 cells once differentiated, a state that implies cell cycle withdrawal (Ruijtenberg and van den Heuvel 2016). As cell cytotoxicity assays, such as Alamar Blue® assay used in this study, depend on cell viability and number, it is unlikely that food-grade TiO_2 particles from the E171 sample directly affects the cell viability of cycling cells but should rather stop their proliferation, similar to the TiO_2 test materials and etoposide. In two previous studies using other TiO_2 nanomodels, no cytotoxicity was observed in proliferating TR146 cells (Teubl et al. 2015a; Teubl et al. 2015b). This discrepancy with the current study may be due to differences between the experimental designs, as viability was assessed 24 h posttreatment by these authors compared to 72 h posttreatment in our study, which allowed more time for cell division. In addition, our conclusion that food-grade TiO_2 mainly impacts cell proliferation is in agreement with a previous study using intestinal Caco-2 cells (enterocytes) exposed to TiO_2 particles (anatase NM100 from the JRC) of which mean size (104 ± 39 nm) was close to that of the E171 sample (105 ± 45 nm) or NM-102 (115 nm)

used in the current study, and viability loss was also reported for only undifferentiated intestinal cells (Vila et al. 2018). Altogether, this corroborates our hypothesis that buccal exposure to food-grade TiO_2 could halt epithelial cell proliferation, suggesting that TiO_2 particle absorption in the human mouth primarily alters epithelium formation or repair rather than directly affecting differentiated epithelial cells. Because active cell division is necessary to ensure the turnover of the buccal mucosa every 14 days (Teubl et al. 2015a), our data raise concerns about E171 exposure that could possibly impact epithelial renewal in the mouth.

The genotoxicity of several sources of TiO_2 NPs, including E171, has been analyzed mainly in intestinal models *in vitro*, and have reported contradictory results. Indeed, it is now well established that NP physicochemical properties (size, shape, surface properties, composition, solubility, aggregation/agglomeration) and experimental conditions greatly influence the cellular genotoxic response (Magdolenova et al. 2014), hampering general conclusions on TiO_2 NP genotoxicity *in vitro*. Our data reveal that E171 and NM-102 with similar particle size distributions (i.e., mostly from 50 to 150 nm) induce DNA damage and slight oxidative stress in TR146 cells contrary to the pure TiO_2-NP particulate model (21 nm). While E171 and TiO_2 from NM-102 contain nano- and submicron-sized particles, in contrast to the TiO_2-NP model, it was suggested that the genotoxic potential of food-grade TiO_2 particles mainly originated for particle with sizes generally above 20 nm. These observations suggest that the nanosized and submicron-sized TiO_2 fractions mixed in the food additive E171 may exert distinct adverse effects on buccal cells, as already reported on intestinal cells (Proquin et al. 2017), and that submicronic particles merit a specific attention when assessing the genotoxicity of E171 in the buccal cavity.

Interestingly, as observed during cytotoxicity testing, we demonstrated that E171 genotoxic activity was higher during TR146 cell proliferation. Similar observations have been reported in intestinal cellular models. Indeed, treating differentiated Caco-2 cells with E171 resulted in DNA base oxidation but not DNA strand breaks after comet assay in its alkaline and Fpg-modified versions (Dorier et al. 2017). On the other hand, undifferentiated proliferating Caco-2 cells exposed to E171 accumulated DNA strand breaks, as assessed by comet assay, but also micronuclei (Proquin et al. 2017). It should be noticed that under our experimental conditions in TR146 proliferating cells, E171 and NM-102 exposure induced DNA strand breaks in alkaline comet assay, but did not result in micronucleus formation. In 2021, EFSA summarized that E171, and more globally TiO_2 NPs, have the potential to induce DNA damage based on *in vitro* and *in vivo* comet assays (Younes et al. 2021). Conversely, EFSA conclusions on the potential of TiO_2 NPs to induce micronuclei were mainly based on *in vivo* assays, as the majority of *in vitro* studies gave negative results. The consequences of DNA damage are detrimental for cycling cells because any DNA lesion may interfere with S-phase progression by blocking the replication fork, eventually leading to fork collapse and the formation of double-strand breaks (Zeman and Cimprich 2014; Kondratick, Washington, and Spies 2020). It should be noted that γH2AX and 53BP1, two markers of DNA double-strand breaks, were activated in proliferating as well as in differentiated TR146 cells, indicating that E171 exposure can primarily induce this type of lesion independent of DNA replication. However, we cannot exclude the possibility that food-grade TiO_2 particle absorption induces other types of lesions, such as DNA base oxidation, as previously reported (Dorier et al. 2017). In TR146 cells exposed to E171, DNA double-strand breaks were more efficiently repaired in differentiated compared to proliferating cells, in which a significant increase of γH2AX staining was maintained several hours after TiO_2 release from the culture medium. Double-strand breaks in noncycling cells are processed by non-homologous end joining which repairs the lesions in less than 1 h, whereas DNA repair in proliferating cells involves different pathways and should be delayed to overcome replication stress (Scully et al. 2019). Because E171-induced CellROX® Green Reagent signal persisted 22 h after wash-out, it was suggested that the TiO_2 particles internalized into the buccal cells lead to ROS formation, perhaps interfering with replication progression and giving rise to late DNA double-strand breaks. It has been proposed that the carcinogenic properties of inhaled TiO_2 rely on genotoxicity through oxidative stress. Animals exposed to TiO_2 NPs *via* inhalation have demonstrated

genotoxic effects in the lungs associated with ROS production, lipid peroxidation and anti-oxidases activation (Sun et al. 2013; Han et al. 2020). On the other hand, *in vivo* testing after TiO_2 ingestion failed to clearly conclude the presence of DNA damage in the intestinal tract (Bettini et al. 2017; Carriere, Arnal, and Douki 2020) despite the induction of oxidative stress (Abbasi-Oshaghi, Mirzaei, and Pourjafar 2019; Zhao et al. 2021). Our results suggest that the food-grade TiO_2 particles from the food additive E171 induce oxidative stress and possibly related DNA damage that at least contributes to cytotoxicity in proliferating cells of the buccal epithelium.

Conclusion

The data presented here provide evidence that under realistic exposure conditions in terms of dose and duration of exposure, food-grade TiO_2 may translocate through the oral mucosa in an *in vivo* pig model of buccal mucosa that is close to the human mouth. We also report the high permeability of human buccal epithelial cells to TiO_2 particles *in vitro*. After these cells were exposed to the food additive for 2 h, TiO_2 particles generated oxidative and genotoxic stresses that were detrimental to proliferating cells mainly. This raises the issue of possible adverse consequences regarding the constant turnover of the buccal mucosa or during wound repair and regeneration. Thus, our study supports that buccal exposure should be considered for TiO_2 risk assessments when being used as a food additive in common foodstuffs, in oral care products such as toothpaste, or as a coating agent in various pharmaceutical drug delivery forms, including those for the sublingual route (European Medicines Agency 2021). To date, because most of the toxicokinetic studies on food-grade TiO_2 have been conducted by gastric gavage, i.e., direct administration into the gastrointestinal tract, the oral cavity is therefore bypassed. However, the buccal epithelium, in addition to the intestine (Teubl et al. 2015a), has to be considered as an additional route for the uptake of food-grade TiO_2, including its nanosized fraction, hence increasing the potential of absorption of foodborne TiO_2 NPs in humans.

Acknowledgements

The authors thank Anne-Marie Cossalter and Mikael Albin for their assistance during animal experiments, and Matthieu Refrégiers for spectrofluorimetry analysis of human saliva.

Author contributions

J.V., A.P.-D., E.G., C.C., P.P., E.B.R., I.-P.O., F.-H.-F.P., B.L., G.M. and E.H. designed the study; E.G., L.D. and N.F. performed physico-chemical characterization of TiO_2 samples; E.G. and P.P. conducted the animal experiments; C.C., C.B. and L.W. performed TEM and SEM-EDX analysis; A.B. and T.T. performed STIM/SIMS (npSCOPE) analysis; J.V., E.B.-R., J.D. and A.P.-D. performed *in vitro* toxicity testings; J.V., A.P.-D., E.G., C.C., A.B., T.T., L.D., J.D., E.B.R., N.F., I.-P.O., F.-H.-F.P., B.L., G.M. and E.H. analyzed the data; J.V., A.B., E.B.R., I.-P.O., F.-H.-F.P., B.L., G.M. and E.H. wrote the paper. All author(s) read and approved the final manuscript.

Disclosure statement

No potential conflict of interest was reported by the author(s).

Funding

The study was supported by INRAE (Institut national de recherche pour l'agriculture, l'alimentation et l'environnement). This work has received fundings from the European Union's Horizon 2020 Research and Innovation Programme under Grant agreement no. 720964 [npSCOPE], by the French National Research Agency (ANR) under Grant number ANR-16-CE34–0011-01 [PAIPITO], and by the Luxembourg National Research Fund via the project INTER/DFG/19/13992454.

Data availability statement

All data generated or analyzed during this study are included in this published article and its supplementary information files.

References

Abbasi-Oshaghi, E., F. Mirzaei, and M. Pourjafar. 2019. "NLRP3 Inflammasome, Oxidative Stress, and Apoptosis Induced in the Intestine and Liver of Rats Treated with Titanium Dioxide Nanoparticles: In Vivo and in Vitro Study." *International Journal of Nanomedicine* 14: 1919–1936. doi:10.2147/IJN.S192382.

Bettini, S., E. Boutet-Robinet, C. Cartier, C. Coméra, E. Gaultier, J. Dupuy, N. Naud, et al. 2017. "Food-Grade TiO2 Impairs Intestinal and Systemic Immune Homeostasis, Initiates Preneoplastic Lesions and Promotes Aberrant

Crypt Development in the Rat Colon." *Scientific Reports* 7: 40373. doi:10.1038/srep40373.

Bischoff, N. S., T. M. de Kok, D. T. H. M. Sijm, S. G. van Breda, J. J. Briedé, J. J. M. Castenmiller, A. Opperhuizen, et al. 2020. "Possible Adverse Effects of Food Additive E171 (Titanium Dioxide) Related to Particle Specific Human Toxicity, Including the Immune System." *International Journal of Molecular Sciences* 22 (1): 207. doi:10.3390/ijms22010207.

Brun, E., F. Barreau, G. Veronesi, B. Fayard, S. Sorieul, C. Chanéac, C. Carapito, et al. 2014. "Titanium Dioxide Nanoparticle Impact and Translocation through ex Vivo, in Vivo and in Vitro Gut Epithelia." *Particle and Fibre Toxicology* 11: 13. doi:10.1186/1743-8977-11-13.

Carriere, M., M.-E. Arnal, and T. Douki. 2020. "TiO2 Genotoxicity: An Update of the Results Published over the Last Six Years." *Mutation Research. Genetic Toxicology and Environmental Mutagenesis* 854-855: 503198. doi:10.1016/j.mrgentox.2020.503198.

Chen, X.-X., B. Cheng, Y.-X. Yang, A. Cao, J.-H. Liu, L.-J. Du, Y. Liu, Y. Zhao, and H. Wang. 2013. "Characterization and Preliminary Toxicity Assay of Nano-Titanium Dioxide Additive in Sugar-Coated Chewing Gum." *Small (Weinheim an Der Bergstrasse, Germany)* 9 (9-10): 1765–1774. doi:10.1002/smll.201201506.

Cho, W.-S., B.-C. Kang, J. K. Lee, J. Jeong, J.-H. Che, and S. H. Seok. 2013. "Comparative Absorption, Distribution, and Excretion of Titanium Dioxide and Zinc Oxide Nanoparticles after Repeated Oral Administration." *Particle and Fibre Toxicology* 10: 9. doi:10.1186/1743-8977-10-9.

Collins, A., P. Møller, G. Gajski, S. Vodenková, A. Abdulwahed, D. Anderson, E. E. Bankoglu, et al. 2023. "Measuring DNA Modifications with the Comet Assay: A Compendium of Protocols." *Nature Protocols* 18 (3): 929–989. doi:10.1038/s41596-022-00754-y.

Coméra, C., C. Cartier, E. Gaultier, O. Catrice, Q. Panouille, S. El Hamdi, K. Tirez, I. Nelissen, V. Théodorou, and E. Houdeau. 2020. "Jejunal Villus Absorption and Paracellular Tight Junction Permeability Are Major Routes for Early Intestinal Uptake of Food-Grade TiO2 Particles: An in Vivo and ex Vivo Study in Mice." *Particle and Fibre Toxicology* 17 (1): 26. doi:10.1186/s12989-020-00357-z.

Commission Regulation (EU) 2022. Commission Regulation (EU) 2022/63 of 14 January 2022 amending Annexes II and III to Regulation (EC) No 1333/2008 of the European Parliament and of the Council as regards the food additive titanium dioxide (E 171).

De Castro, O., A. Biesemeier, E. Serralta, O. Bouton, R. Barrahma, Q. H. Hoang, S. Cambier, et al. 2021. "npSCOPE: A New Multimodal Instrument for in Situ Correlative Analysis of Nanoparticles." *Analytical Chemistry* 93 (43): 14417–14424. doi:10.1021/acs.analchem.1c02337.

Dorier, M., D. Béal, C. Marie-Desvergne, M. Dubosson, F. Barreau, E. Houdeau, N. Herlin-Boime, and M. Carriere. 2017. "Continuous in Vitro Exposure of Intestinal Epithelial Cells to E171 Food Additive Causes Oxidative Stress, Inducing Oxidation of DNA Bases but no Endoplasmic Reticulum Stress." *Nanotoxicology* 11 (6): 751–761. doi:10.1080/17435390.2017.1349203.

Dudefoi, W., H. Terrisse, A. F. Popa, E. Gautron, B. Humbert, and M.-H. Ropers. 2018. "Evaluation of the Content of TiO2 Nanoparticles in the Coatings of Chewing Gums." *Food Additives & Contaminants. Part A, Chemistry, Analysis, Control, Exposure & Risk Assessment* 35 (2): 211–221. doi:10.1080/19440049.2017.1384576.

EFSA Panel on Food Additives and Nutrient Sources added to Food (ANS), 2016. "Re-Evaluation of Titanium Dioxide (E 171) as a Foodadditive." *EFSA Journal. European Food Safety Authority* 14 (9): 4545.

European Medicines Agency 2021. Final Feedback from European Medicine Agency (EMA) to the EU Commission Request to Evaluate the Impact of the Removal of Titanium Dioxide from the List of Authorised Food Additives on Medicinal Products.

Fernandez-Vidal, A., J. Vignard, and G. Mirey. 2017. "Around and beyond 53BP1 Nuclear Bodies." *International Journal of Molecular Sciences* 18 (12): 2611. doi:10.3390/ijms18122611.

Fiordaliso, F., C. Foray, M. Salio, M. Salmona, and L. Diomede. 2018. "Realistic Evaluation of Titanium Dioxide Nanoparticle Exposure in Chewing Gum." *Journal of Agricultural and Food Chemistry* 66 (26): 6860–6868. doi:10.1021/acs.jafc.8b00747.

Guillard, A., E. Gaultier, C. Cartier, L. Devoille, J. Noireaux, L. Chevalier, M. Morin, et al. 2020. "Basal Ti Level in the Human Placenta and Meconium and Evidence of a Materno-Foetal Transfer of Food-Grade TiO2 Nanoparticles in an ex Vivo Placental Perfusion Model." *Particle and Fibre Toxicology* 17 (1): 51. doi:10.1186/s12989-020-00381-z.

Han, B., Z. Pei, L. Shi, Q. Wang, C. Li, B. Zhang, X. Su, et al. 2020. "TiO2 Nanoparticles Caused DNA Damage in Lung and Extra-Pulmonary Organs through ROS-Activated FOXO3a Signaling Pathway after Intratracheal Administration in Rats." *International Journal of Nanomedicine* 15: 6279–6294. doi:10.2147/IJN.S254969.

Heringa, M. B., L. Geraets, J. C. H. van Eijkeren, R. J. Vandebriel, W. H. de Jong, and A. G. Oomen. 2016. "Risk Assessment of Titanium Dioxide Nanoparticles via Oral Exposure, Including Toxicokinetic Considerations." *Nanotoxicology* 10 (10): 1515–1525. doi:10.1080/17435390.2016.1238113.

Heringa, M. B., R. J. B. Peters, R. L a W. Bleys, M. K. van der Lee, P. C. Tromp, P. C. E. van Kesteren, J. C. H. van Eijkeren, A. K. Undas, A. G. Oomen, and H. Bouwmeester. 2018. "Detection of Titanium Particles in Human Liver and Spleen and Possible Health Implications." *Particle and Fibre Toxicology* 15 (1): 15. doi:10.1186/s12989-018-0251-7.

Jones, K., J. Morton, I. Smith, K. Jurkschat, A.-H. Harding, and G. Evans. 2015. "Human in Vivo and in Vitro Studies on Gastrointestinal Absorption of Titanium Dioxide Nanoparticles." *Toxicology Letters* 233 (2): 95–101. doi:10.1016/j.toxlet.2014.12.005.

Kondratick, C. M., M. T. Washington, and M. Spies. 2020. "Making Choices: DNA Replication Fork Recovery Mechanisms." *Seminars in Cell & Developmental Biology* S1084-9521 (20): 30122.

Kreyling, W. G., U. Holzwarth, C. Schleh, J. Kozempel, A. Wenk, N. Haberl, S. Hirn, et al. 2017. "Quantitative Biokinetics of Titanium Dioxide Nanoparticles after Oral Application in Rats: Part 2." *Nanotoxicology* 11 (4): 443–453. doi:10.1080/17435390.2017.1306893.

Lagerlöf, F., and C. Dawes. 1984. "The Volume of Saliva in the Mouth before and after Swallowing." *Journal of Dental Research* 63 (5): 618–621. doi:10.1177/00220345840630050201.

Madhav, N. V. S., A. K. Shakya, P. Shakya, and K. Singh. 2009. "Orotransmucosal Drug Delivery Systems: A Review." *Journal of Controlled Release : official Journal of the Controlled Release Society* 140 (1): 2–11. doi:10.1016/j.jconrel.2009.07.016.

Magdolenova, Z., A. Collins, A. Kumar, A. Dhawan, V. Stone, and M. Dusinska. 2014. "Mechanisms of Genotoxicity. A Review of in Vitro and in Vivo Studies with Engineered Nanoparticles." *Nanotoxicology* 8 (3): 233–278. doi:10.3109/17435390.2013.773464.

Medina-Reyes, E. I., N. L. Delgado-Buenrostro, D. Díaz-Urbina, C. Rodríguez-Ibarra, A. Déciga-Alcaraz, M. I. González, J. L. Reyes, et al. 2020. "Food-Grade Titanium Dioxide (E171) Induces Anxiety, Adenomas in Colon and Goblet Cells Hyperplasia in a Regular Diet Model and Microvesicular Steatosis in a High Fat Diet Model." *Food and Chemical Toxicology : An International Journal Published for the British Industrial Biological Research Association* 146: 111786. doi:10.1016/j.fct.2020.111786.

Ng, S. L., S. Das, Y.-P. Ting, R. C. W. Wong, and N. Chanchareonsook. 2021. "Benefits and Biosafety of Use of 3D-Printing Technology for Titanium Biomedical Implants: A Pilot Study in the Rabbit Model." *International Journal of Molecular Sciences* 22 (16): 8480. doi:10.3390/ijms22168480.

Nielsen, H. M., and M. R. Rassing. 2000. "TR146 Cells Grown on Filters as a Model of Human Buccal Epithelium: IV. Permeability of Water, Mannitol, Testosterone and Beta-Adrenoceptor Antagonists. Comparison to Human, Monkey and Porcine Buccal Mucosa." *International Journal of Pharmaceutics* 194 (2): 155–167. doi:10.1016/s0378-5173(99)00368-3.

Onodera, K., K. Ooya, and H. Kawamura. 1993. "Titanium Lymph Node Pigmentation in the Reconstruction Plate System of a Mandibular Bone Defect." *Oral Surgery, Oral Medicine, and Oral Pathology* 75 (4): 495–497. doi:10.1016/0030-4220(93)90177-6.

Palugan, L., M. Spoldi, F. Rizzuto, N. Guerra, M. Uboldi, M. Cerea, S. Moutaharrik, A. Melocchi, A. Gazzaniga, and L. Zema. 2022. "What's Next in the Use of Opacifiers for Cosmetic Coatings of Solid Dosage Forms? Insights on Current Titanium Dioxide Alternatives." *International Journal of Pharmaceutics* 616: 121550. doi:10.1016/j.ijpharm.2022.121550.

Peters, R. J. B., A. G. Oomen, G. van Bemmel, L. van Vliet, A. K. Undas, S. Munniks, R. L. A. W. Bleys, P. C. Tromp, W. Brand, and M. van der Lee. 2020. "Silicon Dioxide and Titanium Dioxide Particles Found in Human Tissues." *Nanotoxicology* 14 (3): 420–432. doi:10.1080/17435390.2020.1718232.

Proquin, H., C. Rodríguez-Ibarra, C. G. J. Moonen, I. M. Urrutia Ortega, J. J. Briedé, T. M. de Kok, H. van Loveren, and Y. I. Chirino. 2017. "Titanium Dioxide Food Additive (E171) Induces ROS Formation and Genotoxicity: contribution of Micro and Nano-Sized Fractions." *Mutagenesis* 32 (1): 139–149. doi:10.1093/mutage/gew051.

Roblegg, E., E. Fröhlich, C. Meindl, B. Teubl, M. Zaversky, and A. Zimmer. 2012. "Evaluation of a Physiological in Vitro System to Study the Transport of Nanoparticles through the Buccal Mucosa." *Nanotoxicology* 6 (4): 399–413. doi:10.3109/17435390.2011.580863.

Ruijtenberg, S., and S. van den Heuvel. 2016. "Coordinating Cell Proliferation and Differentiation: Antagonism between Cell Cycle Regulators and Cell Type-Specific Gene Expression." *Cell Cycle (Georgetown, Tex.)* 15 (2): 196–212. doi:10.1080/15384101.2015.1120925.

Scully, R., A. Panday, R. Elango, and N. A. Willis. 2019. "DNA Double-Strand Break Repair-Pathway Choice in Somatic Mammalian Cells." *Nature Reviews, Molecular Cell Biology* 20 (11): 698–714. doi:10.1038/s41580-019-0152-0.

Sun, L., Wu, J. Du, F. Chen, X. and Chen, Z. J. 2013. "Cyclic GMP-AMP Synthase is a Cytosolic DNA Sensor That Activates the Type I Interferon Pathway." *Science (New York, N.Y.)* 339 (6121): 786–791. doi:10.1126/science.1232458.

Teubl, B. J., M. Absenger, E. Fröhlich, G. Leitinger, A. Zimmer, and E. Roblegg. 2013. "The Oral Cavity as a Biological Barrier System: design of an Advanced Buccal in Vitro Permeability Model." *European Journal of Pharmaceutics and Biopharmaceutics : official Journal of Arbeitsgemeinschaft Fur Pharmazeutische Verfahrenstechnik e.V* 84 (2): 386–393. doi:10.1016/j.ejpb.2012.10.021.

Teubl, B. J., G. Leitinger, M. Schneider, C.-M. Lehr, E. Fröhlich, A. Zimmer, and E. Roblegg. 2015a. "The Buccal Mucosa as a Route for TiO2 Nanoparticle Uptake." *Nanotoxicology* 9 (2): 253–261. doi:10.3109/17435390.2014.921343.

Teubl, B. J., C. Schimpel, G. Leitinger, B. Bauer, E. Fröhlich, A. Zimmer, and E. Roblegg. 2015b. "Interactions between nano-TiO2 and the Oral Cavity: impact of Nanomaterial Surface Hydrophilicity/Hydrophobicity." *Journal of Hazardous Materials* 286: 298–305. doi:10.1016/j.jhazmat.2014.12.064.

Urrutia-Ortega, I. M., L. G. Garduño-Balderas, N. L. Delgado-Buenrostro, V. Freyre-Fonseca, J. O. Flores-Flores, A. González-Robles, J. Pedraza-Chaverri, et al. 2016. "Food-Grade Titanium Dioxide Exposure Exacerbates Tumor Formation in Colitis Associated Cancer Model." *Food and Chemical Toxicology : An International Journal Published for the British Industrial Biological Research Association* 93: 20–31. doi:10.1016/j.fct.2016.04.014.

Vignard, J., G. Mirey, and B. Salles. 2013. "Ionizing-Radiation Induced DNA Double-Strand Breaks: A Direct and Indirect Lighting up." *Radiotherapy and Oncology : journal of the European Society for Therapeutic Radiology and Oncology* 108 (3): 362–369. doi:10.1016/j.radonc.2013.06.013.

Vila, L., A. García-Rodríguez, R. Marcos, and A. Hernández. 2018. "Titanium Dioxide Nanoparticles Translocate through Differentiated Caco-2 Cell Monolayers, without Disrupting the Barrier Functionality or Inducing Genotoxic Damage." *Journal of Applied Toxicology : JAT* 38 (9): 1195–1205. doi:10.1002/jat.3630.

Watanabe, Shigeru, Y. Yamamura, A. Hoshiai, S. Morishita, A. Machiya, S. Matsuda, T. Shimojima, and I. Tohnai. 2021. "Salivary Volume in the Mouth Immediately before and after Swallowing in Children." *Dental, Oral and Maxillofacial Research* 7 (1): 3. doi:10.15761/DOMR.1000377.

Weingart, D., S. Steinemann, W. Schilli, J. R. Strub, U. Hellerich, J. Assenmacher, and J. Simpson. 1994. "Titanium Deposition in Regional Lymph Nodes after Insertion of Titanium Screw Implants in Maxillofacial Region." *International Journal of Oral and Maxillofacial Surgery* 23 (6 Pt 2): 450–452. doi:10.1016/s0901-5027(05)80045-1.

Weir, A., P. Westerhoff, L. Fabricius, K. Hristovski, and N. von Goetz. 2012. "Titanium Dioxide Nanoparticles in Food and Personal Care Products." *Environmental Science & Technology* 46 (4): 2242–2250. doi:10.1021/es204168d.

Younes, M., G. Aquilina, L. Castle, K.-H. Engel, P. Fowler, M. J. Frutos Fernandez, P. Fürst, EFSA Panel on Food Additives and Flavourings (FAF), et al. 2021. "Safety assessment of titanium dioxide (E171) as a food additive." *EFSA journal. European Food Safety Authority* 19 (5): e06585. doi:10.2903/j.efsa.2021.6585.

Zeman, M. K., and K. A. Cimprich. 2014. "Causes and Consequences of Replication Stress." *Nature Cell Biology* 16 (1): 2–9. doi:10.1038/ncb2897.

Zhao, Y., Y. Tang, S. Liu, T. Jia, D. Zhou, and H. Xu. 2021. "Foodborne TiO2 Nanoparticles Induced More Severe Hepatotoxicity in Fructose-Induced Metabolic Syndrome Mice via Exacerbating Oxidative Stress-Mediated Intestinal Barrier Damage." *Foods (Basel, Switzerland)* 10 (5): 986. doi:10.3390/foods10050986.